*Nucleic Acids Research, 2005, Vol. 33, No. 3* ***1031–1039***
*doi:10.1093/nar/gki253*

# 8-vinyl-deoxyadenosine, an alternative fluorescent nucleoside analog to 2′-deoxyribosyl-2-aminopurine with improved properties

**Nouha Ben Gaied, Nicole Glasser[1], Nick Ramalanjaona[1], Hervé Beltz[1], Philippe Wolff[2], Roland Marquet[2], Alain Burger and Yves Mély[1,*]**

Laboratoire de Chimie Bioorganique, UMR 6001 du CNRS, Université de Nice Sophia Antipolis Parc Valrose, 06108 Nice cedex 2, France, [1]Laboratoire de Pharmacologie et Physico-chimie des interactions cellulaires et moléculaires, UMR 7034 du CNRS, Faculté de Pharmacie, Université Louis Pasteur, 74 Route du Rhin, BP 24, 67401 Illkirch cedex, France and [2]Laboratoire de Structure des Macromolécules Biologiques et Mécanismes de Reconnaissance, UPR 9002 du CNRS conventionnée à l'Université Louis Pasteur, 15 rue René Descartes, 67084 Strasbourg cedex, France

Received October 26, 2004; Revised and Accepted January 27, 2005

## ABSTRACT

**We report here the synthesis and the spectroscopic characterization of 8-vinyl-deoxyadenosine (8vdA), a new fluorescent analog of deoxyadenosine. 8vdA was found to absorb and emit in the same wavelength range as 2′-deoxyribosyl-2-aminopurine (2AP), the most frequently used fluorescent nucleoside analog. Though the quantum yield of 8vdA is similar to that of 2AP, its molar absorption coefficient is about twice, enabling a more sensitive detection. Moreover, the fluorescence of 8vdA was found to be sensitive to temperature and solvent but not to pH (around neutrality) or coupling to phosphate groups. Though 8vdA is base sensitive and susceptible to depurination, the corresponding phosphoramidite was successfully prepared and incorporated in oligonucleotides of the type d(CGT TTT XNX TTT TGC) where N = 8vdA and X = A, T or C. The 8vdA-labeled oligonucleotides gave more stable duplexes than the corresponding 2AP-labeled sequences when X = A or T, indicating that 8vdA is less perturbing than 2AP and probably adopts an *anti* conformation to preserve the Watson–Crick H-bonding. In addition, the quantum yield of 8vdA is significantly higher than 2AP in all tested oligonucleotides in both their single strand and duplex states. The steady-state and time-resolved fluorescence parameters of 8vdA and 2AP were found to depend similarly on the nature of their flanking residues and on base pairing, suggesting that their photophysics are governed by similar mechanisms. Taken together, our data suggest that 8vdA is a non perturbing nucleoside analog that may be used with improved sensitivity for the same applications as 2AP.**

## INTRODUCTION

Fluorescent nucleoside analogs that minimally disturb the structure and function of nucleic acids are of major interest for studying the structure, the dynamics and the interactions of nucleic acids with their molecular targets (1). Among them, 2′-deoxyribosyl-2-aminopurine (2AP) (Figure 1) is the most popular. 2AP has a very high quantum yield (0.68) at physiological pH and a low excitation energy as compared to the natural nucleic acid bases and protein amino acids and can

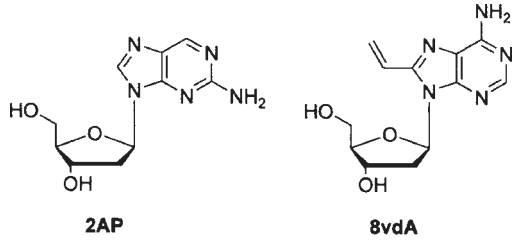


**Figure 1.** Structures of 2AP and 8vdA.

*To whom correspondence should be addressed. Tel: +33 3 90 24 42 63; Fax: +33 3 90 24 43 12; Email: mely@aspirine.u-strasbg.fr
Correspondence may also be addressed to Alain Burger. Tel: +33 4 92 07 61 53; Fax: +33 4 92 07 61 51; Email: burger@unice.fr

The authors wish it to be known that, in their opinion, the first two authors should be regarded as joint First Authors

therefore be selectively excited (2). 2AP is also able to establish stable Watson–Crick interactions with thymine, preserving the normal B-form of DNA (3–6). Furthermore, using solid phase synthesis and phosphoramidite chemistry, it can substitute adenosines at any selected position in oligonucleotides. Due to these characteristics, 2AP has been largely used to probe the dynamics of melting (3,7), abasic sites (8,9), mismatched base pairs (10), metal ion binding (9,11) and the thermodynamics and kinetics of protein-induced DNA conformational transitions (2,3,7,12–19) as well as RNA–RNA complex formation (20,21). However, when 2AP is incorporated into single or double stranded oligonucleotides, its fluorescence quantum yield is reduced up to 100-fold, requiring thus high concentrations of 2AP-labeled oligonucleotides. Consequently, there is a strong demand for new nucleoside analogs with improved spectroscopic properties.

Here, we report the synthesis of the 8-vinyldeoxyadenosine phosphoramidite monomer and its incorporation into oligonucleotides using solid phase automated DNA synthesis. Although, it is known that the introduction of a substituent at C-8 of the base modifies the *syn-anti* equilibrium and drives the equilibrium to the less favorable *syn* isomer (22), the equilibrium is not completely shifted to the *syn* conformation in case of medium sized substituents and the nucleotide analog can accommodate the *anti* conformation in duplexes (23–26). In addition, in duplexes containing 8-vinyldeoxyadenosine (8vdA) (Figure 1), the vinyl group might improve base stacking when exposed into the major groove, and thus contribute to the duplex stability (27,28). The fluorescence properties of the monomer, as well as their dependence on pH, temperature, solvent and coupling to phosphate group were characterized. In addition, the fluorescence properties of 8vdA and 2AP were further compared in the single-strand and duplex states of three 15mer oligonucleotides differing by the nature of the closest neighbors to the fluorescent analog. The thermodynamic stability and pairing selectivity were also investigated in matched and mismatched duplexes and compared with that of the corresponding duplexes containing deoxyadenosine. Our data show that 8vdA can advantageously replace 2AP in nucleic acids for fluorescence studies.

## MATERIALS AND METHODS

### Synthesis of 8vdA and oligonucleotides

The synthesis of 5′-dimethoxytrityl-8-vinyl-2′-deoxyadenosine (**4**), 5′-Dimethoxytrityl-6-*N*,*N*-dimethylformamidine-8-vinyl-2′-deoxyadenosine (**5**) and 3′-*N*,*N*′-diisopropylcyanoethylphosphoramidite-5′-dimethoxytrityl-6-*N*,*N*-dimethylformamidine-8-vinyl-2′-deoxyadenosine (**6**), and solid phase oligonucleotide synthesis are described in the Supplementary Material.

### Spectroscopic measurements

Absorption spectra were recorded in a Peltier thermostated cell holder on a Cary 400 spectrophotometer. Melting curves were recorded by following the temperature-dependence of the absorbance changes of a 450–700 nM oligonucleotide concentration. The melting curves were converted into an $\alpha$ versus $T$ profile, where $\alpha$ represents the fraction of single-strands in the duplex state (29). From this profile, assuming a two-state reaction, the van't Hoff transition enthalpy $\Delta H^0$ was calculated using the expression:

$$\Delta H^0 = 6RT_m^2 \left(\frac{\partial \alpha}{\partial T}\right)_{T_m}, \quad \mathbf{1}$$

where $\left(\frac{\partial \alpha}{\partial T}\right)_{T_m}$ is the slope of the transition at the melting temperature. The entropy change, $\Delta S^0$ was then determined from:

$$\Delta S^0 = \frac{\Delta H^0}{T_m} + R \ln\left(\frac{4}{C_T}\right), \quad \mathbf{2}$$

where $C_T$ is the total concentration of strands (the concentration of the two strands being equal). Finally, the free energy change, $\Delta G^0_{37}$, at 37°C is calculated by: $\Delta G^0_{37} = \Delta H^0 - T\Delta S^0$.

Steady-state fluorescence measurements were performed on a Fluoromax 3 spectrofluorometer. Quantum yields were determined relative to 2-aminopurine in water ($\phi$ = 0.68) (2). Free 8vdA was dissolved in HEPES buffer 25 mM, pH 7.5 at 20°C. 8vdA- and 2AP-labeled oligonucleotides were dissolved in HEPES buffer 25 mM, NaCl 30 mM and $MgCl_2$ 0.2 mM, pH 7.5. The experimental radiative rate constant, $k_r$, and nonradiative rate constant, $k_{nr}$, were determined by $k_r = \phi/\langle\tau\rangle$ and $k_{nr} = (1-\phi)/\langle\tau\rangle$, respectively, where $\langle\tau\rangle$ is the average lifetime.

The pH effect on 8vdA fluorescence intensity was studied by using different buffers: *N*-*N*′-diethyl-*N*-*N*′-bis(sulfopropyl)-ethylene-diamine (Despen) for pH < 6, 2-(*N*-morpholino)-ethane sulfonic acid (Mes) for 6 < pH < 7, *N*-(2-hydroxyethyl)-piperazine-*N*′-2-ethane sulfonic acid (HEPES) for 7 < pH < 9 and finally 2-(*N*-cyclohexylamino)-ethane sulfonic acid (Ches) at pH > 9. The temperature effect was monitored in HEPES buffer 25 mM, NaCl 30 mM and $MgCl_2$ 0.2 mM, pH 7.5 by following the fluorescence intensity at the maximum emission wavelength between 10 and 60°C.

Time-resolved fluorescence measurements were carried out with the single-photon counting time-correlated technique, using a pulse-picked frequency tripled Ti-sapphire laser (Tsunami, Spectra Physics) as described previously(30). Excitation was at 295 nm. Emission was at 380 nm. Time-resolved data analysis was performed using the maximum entropy method (MEM) and the Pulse5 software (31). In all cases, the $\chi^2$ values were close to 1.0, and the weighted residuals as well as the autocorrelation of the residuals were randomly distributed around zero indicating an optimal fit.

## RESULTS

### Synthesis of phosphoramidite 6 and 8vdA-labeled oligonucleotides

The synthesis of the phosphoramidite **6** and the 8vdA-labeled oligonucleotides needed to be addressed adequately due to the intrinsic sensitivity of the modified base to basic and acidic conditions (32–35). These limiting factors were taken into account in our synthetic approach to obtain oligonucleotides of the highest purity for spectroscopic studies.

The synthesis of the phosphoramidite of 8vdA **6** is described in Figure 2. The synthesis of 8vdA and of the 5′-diphosphate derivative was described previously (33,35). Compound **3** was

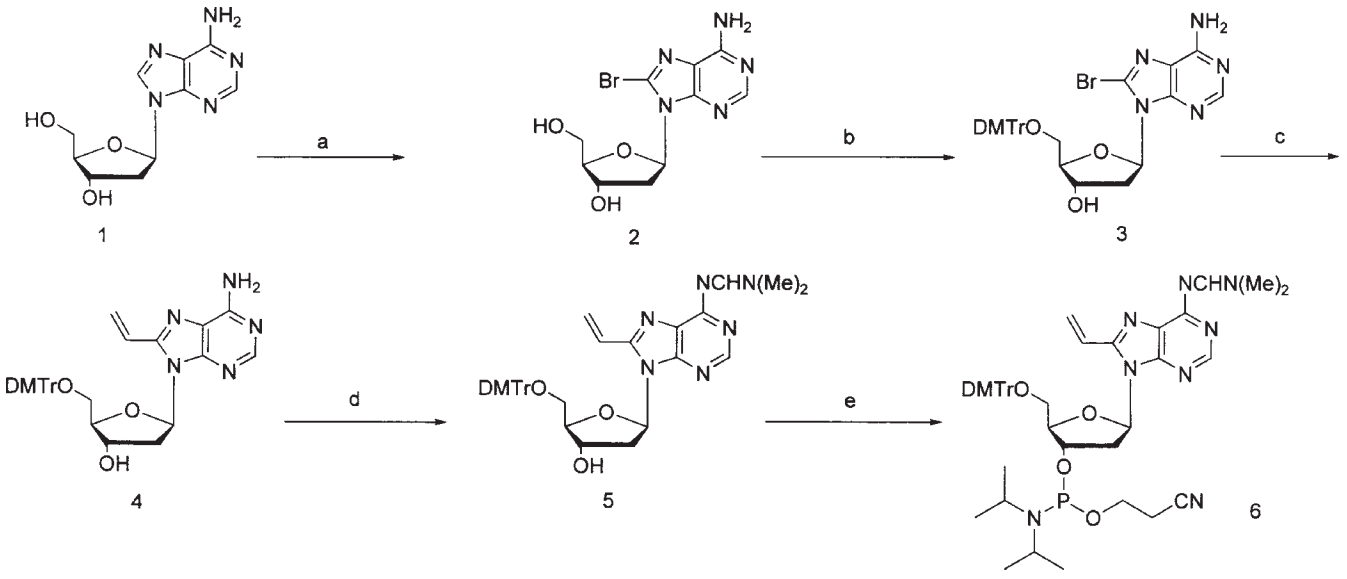


**Figure 2.** Synthesis of the 8-vinyl-2′-deoxyadenosine phosphoramidite (**6**). (a) $Br_2$, acetate buffer, pH 4.2 (72%); (b) DMTrCl, $DMAP_{cat}$, pyridine (87%); (c) $Pd(PPh_3)_4$, $Sn(CH{=}CH_2)_4$, NMP, 110°C (82%); (d) $Me_2NCH(OMe)_2$, MeOH (93%) and (e) $CN(CH_2)_2OP[N(iPr)_2]_2$, tetrazole, $CH_2Cl_2$ (60%).

prepared according to the literature (36,37). Subsequently, the vinyl moiety was introduced via a Stille coupling using $Pd(PPh_3)_4$ as catalyst and tetravinyltin. The last step before reaching the phosphoramidite monomer was to protect the exocyclic amine with the dimethylformamidine group. This protecting group was preferred to the benzoyl group because it imparts depurination resistance (38) under acidic detritylation conditions (38–40) and is rapidly deprotected during the ammonia treatment used in oligonucleotide synthesis (*vide infra*) (38). The phosphoramidite **6** was finally obtained in satisfactory yield using preferentially the *N*,*N*′-diisopropylcyanoethylphosphorodiamidite instead of the chloride phosphoramidite to avoid side reactions (35).

Following the preparation of phosphoramidite **6**, the solid phase synthesis of different sequences was undertaken. In order to obtain oligomers of the highest purity, several parameters were modified in the standard protocol. Preliminary studies with 8vdA showed that the base was quite stable in concentrated ammonia (28%) for a short reaction time, but on prolonged reaction time gave a more polar compound that accumulated as evidenced by thin layer chromatography and UV. Thus, to limit the reaction of 8vdA with ammonia, fast-deprotecting building blocks were preferred. We used dichloroacetic acid (3%) to reduce depurination during detritylation (41). To ensure high coupling yield (>97%), coupling was run for 35 s when the building block **6** was employed. $Pac_2O$ in cap A was used instead of $Ac_2O$ to avoid the formation of dG-$N_6$ acetylated derivatives (39,42–44). We also replaced the oxidizing agent normally used in solid phase synthesis ($I_2$/Pyridin/$H_2O$) by the commercially available ethyl (methyl)dioxirane. This new efficient reagent can be applied to both solid and solution phase with either N-protected or N-unprotected nucleosides under very fast non-basic anhydrous conditions (45) and is more compatible with the formamidine protecting group (38,46). Under these conditions, the average coupling yield per step was >97%.

Deprotection in ammonia (28%) at room temperature was studied at different times with the 8vdA-labeled ODN3 sequence by ion exchange high-performance liquid chromatography (HPLC) and matrix-assisted laser desorption ionization time-of-flight mass spectrometry (MALDI-TOF MS). HPLC of the crude product obtained after 4 h treatment showed one major compound and a minor compound eluting before the expected oligonucleotide. When deprotection lasted 24 h, the ratio of the two products was reversed (Supplementary Figure 7). MS analysis of the slower eluting product gave the correct molecular weight whereas the faster eluting compound gave a molecular weight with a mass difference ($\Delta M$) of 17. The latter compound might result from the addition of ammonia on the vinyl moiety. These data indicate that prolonged deprotection time is detrimental. Thus, we retained 4 h ammonia treatment for the other sequences (Supplementary Figure 8). Attempts using mild deprotecting conditions ($K_2CO_3$/MeOH) (42) were unsatisfactory even after 24 h. After 4 h ammonia treatment, the oligomers were purified by ion exchange HPLC and characterized by MS. The synthesis of the 8vdA-labeled 15mer with X = G was also tried. However in this case, MS analysis afforded an *m*/*z* for the major compound exceeding the expected mass ($\Delta M$ = +151 and +174). These mass differences are compatible with guanine and guanine/sodium adducts, respectively. This product might arise from nucleophilic addition of dG phosphoramidate (N-7) on the vinyl group of 8vdA during the coupling step. A similar problem was described with 6-vinylpurine nucleoside (47) and illustrates the limitation of the synthetic approach used here.

## Conformational analysis of 8vdA

The 8-vinyl derivative **4** was analyzed by 1D and 2D (COSY, NOESY) $^1$H NMR at 300K and compared with 5′-DMT-dA (Supplementary Figures 9 and 10). Analysis of the $^3$J coupling constants (48) of the deoxyribose moiety (Supplementary Material) showed that the sugar ring is biased towards the South conformation with a comparable magnitude as measured for 5′-DMT-deoxyadenosine (>60%). The $^3$J coupling data indicate that the vinyl group has little impact on the

repartition of the North and South conformer population. We also examined the influence of the vinyl substituent on the *syn–anti* equilibrium of the base by NOESY. The *syn* and *anti* conformations were qualitatively deduced from the correlations between the internal vinylic proton and H-1′ and H-2′ (49). The NOESY study of compound **4** showed that the base was not locked in the *syn* conformation and that both the *syn* and *anti* conformations were present.

## Spectroscopic properties of 8vdA

In the first step, the absorption and emission properties of 8vdA in 25 mM HEPES buffer, pH 7.5 were determined and compared to those of the reference compound, 2AP.

The absorption, excitation and emission spectra of 8vdA at room temperature are shown in Figure 3. 8vdA exhibits a broad absorption spectrum, with a maximum absorption wavelength at 290 nm, close to that of 2AP (303 nm). Since 8vdA could be excited up to 340 nm, similar to 2AP, it could be selectively excited without interfering with natural bases and amino acids, allowing observations of protein/oligonucleotide interactions when 8vdA is excited. Though the absorption properties of the two nucleosides are qualitatively similar, they differ quantitatively since the absorption coefficient of 8vdA (12 600 $M^{-1}cm^{-1}$) (33) is about twice that of 2AP (7200 $M^{-1}cm^{-1}$). The absorption and excitation spectra are largely superimposable, suggesting that fluorescent impurities are minimal. The fluorescence spectrum consists of a broad structureless band with a maximum emission wavelength at 382 nm, shifted to the red as compared to 2AP (370 nm). It follows that 8vdA exhibits a Stokes shift of 92 nm (8300 $cm^{-1}$) much larger than that of 2 AP, which is only of 67 nm (5970 $cm^{-1}$) (Table 1). The quantum yield at 25°C is 0.65 (±0.01) and is independent of the excitation wavelength in the 260–310 nm region, confirming that fluorescence contaminants are negligible. The quantum yield of 8vdA is similar to that of 2AP (0.68) and is thus much higher than the quantum yield of other fluorescent nucleotide analogs like formycin or 2,6-diaminopurine which are below 0.1 (2). Since the extinction coefficient of 8vdA is about twice that of 2AP, it follows that 8vdA can be detected twice more sensitively by fluorescence than 2AP.

The fluorescent intensity decay of 8vdA is exponential with a 4.7 ns lifetime that is significantly less than the 10.4 ns lifetime of 2AP (Table 1) (10). It follows that the radiative rate constant, $k_r = 1.4 \times 10^8\ s^{-1}$, of 8vdA is about twice that of 2AP ($k_r = 6.5 \times 10^7\ s^{-1}$). To get further information on 8vdA photophysics, the influence of various physico-chemical parameters was investigated. In Figure 4, the pH dependence of the fluorescence intensity is reported. Similar to 2AP, the fluorescence intensity of 8vdA is constant in the pH range 5–10, where the chromophore is neutral. At a pH below 5 or above 10, the intensity decreases without any maximum emission

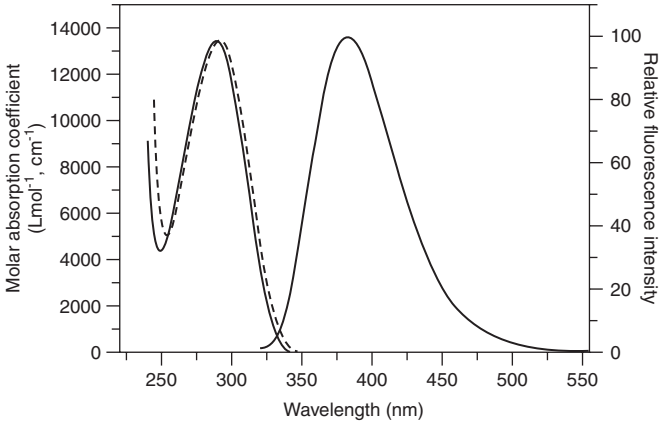


**Figure 3.** Absorption and emission spectra of 8vdA. The free 8vdA deoxyribonucleoside was dissolved in HEPES 25 mM, pH 7.5. The excitation spectrum (dotted line) was recorded at an emission wavelength of 380 nm. The emission spectrum (solid line) was recorded at an excitation wavelength of 305 nm.

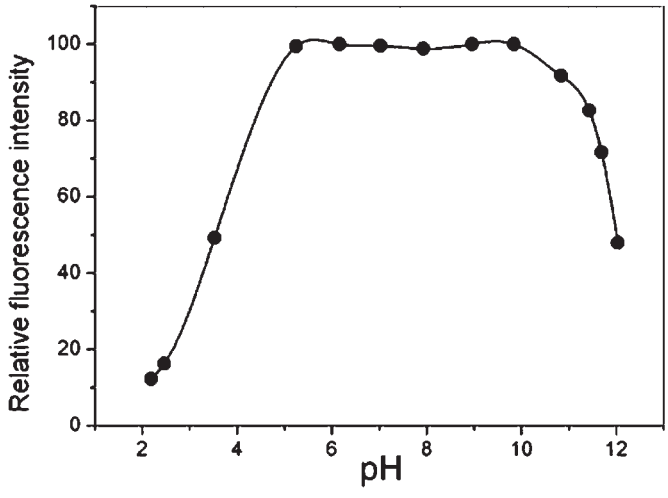


**Figure 4.** pH dependence of the fluorescence of 8vdA. A concentration of 7.5 µM of 8vdA was dissolved either in Despen, MES, HEPES, or CHES as described under Materials and Methods. It was checked at overlapping pH values that the fluorescence intensity does not depend on the buffer nature. Excitation and emission wavelengths were 305 and 380 nm, respectively.

**Table 1.** Steady-state and time-resolved fluorescence parameters of 8vdA

| | $\lambda_{max}$ abs (nm) | $\lambda_{max}$ em (nm) | $\phi \pm 0.02$ (25°C) | $\tau \pm 0.1$ ns (25°C) | $k_r$ ($10^7\ s^{-1}$) $\pm 0.5 \times 10^7$ | $k_{nr}$ ($10^7\ s^{-1}$) $\pm 0.5 \times 10^7$ |
|---|---|---|---|---|---|---|
| 8vdA in HEPES | 290 | 382 | 0.66 | 4.7 | 14.0 | 7.2 |
| 2AP in water[a] | 303 | 370 | 0.68 | 10.4[b] | 6.5 | 3.1 |
| 8vdA in methanol | 294 | 375 | 0.32 | 2.9 | 11.0 | 23.5 |
| 8vAdiP in HEPES[c] | 292 | 382 | 0.64 | 4.9 | 13.1 | 7.4 |
| 8vAdiP in methanol[c] | 293 | 378 | 0.26 | 2.4 | 10.8 | 30.8 |

[a]Data from (2).
[b]Data from (10).
[c]8vAdiP designates the 8vA base with a diphosphate group on the ribosyl 5′-OH group.

wavelength shift. A pK value in the excited state of 3.7 (±0.1), close to that of 2AP, was obtained from the fluorescence decrease in the acidic pH range (2). In the next step, the temperature dependence of fluorescence intensity was studied over 10–60°C. When the temperature increases, a simultaneous decrease in the quantum yield and the fluorescence lifetime is observed. The quantum yield decreases from 0.71 at 10°C to 0.52 at 60°C and the lifetime from 5 to 3.3 ns, while the shape of the emission spectrum is unaffected by temperature. The parallel decrease of the quantum yield and lifetime indicates that as expected, the radiative rate constant is independent of the temperature. In Figure 5, the inverse of the lifetime was plotted as a function of the inverse of the temperature in an Arrhenius plot. The experimental data were fitted with the equation:

$$\frac{1}{\tau} = k_0 + A\,e^{-E_a/RT}, \qquad \mathbf{3}$$

where $k_0$ is the temperature-independent rate constant, $A$ is the nonradiative thermal pre-exponential factor, $E_a$ is the activation energy for thermal quenching, $R$ is the gas constant and $T$ is the absolute temperature. The $k_0$ value was found to be $1.9 \times 10^8$ s$^{-1}$. This value is slightly higher than the $k_r$ value ($1.4 \times 10^8$ s$^{-1}$), suggesting that the radiative rate constant is probably not the only temperature independent pathway but it is the dominant one. The activation energy and the A factor were found to be 8.8 kcal/mol and $6.1 \times 10^{13}$ s$^{-1}$, respectively.

In an additional step, the effect of the polarity was tested on 8vdA. To this end, we dissolved 8vdA in methanol and compared its spectroscopic properties with those in water. We observe a 7 nm blue-shift in the emission maximum as compared with water, a value close to that observed with 2AP. Since in addition, there is a 4 nm red-shift in absorption, it results that the Stokes shift strongly decreases in methanol (7350 cm$^{-1}$). Moreover, the quantum yield decreases by 50% and the fluorescence lifetime drops to 2.9 ns (Table 1). Since the $k_r$ value ($1.1 \times 10^8$ s$^{-1}$) in methanol is close to that in water, it results that the decrease of the fluorescence parameters ($\phi$ and $\tau$) in methanol with respect to water are mainly due to an increase in the nonradiative rate constant.

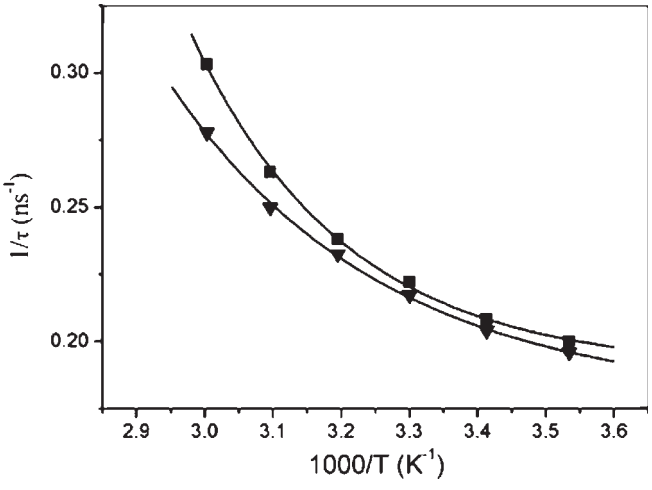


**Figure 5.** Temperature dependence of the lifetime of 8vdA in its free (solid square) and phosphorylated (solid inverted triangle) forms. The data were fitted with Equation 3 using the data reported in the text.

Finally, the effect of the introduction of a phosphate group on the ribosyl 5′-OH group was evaluated. As in the case of 2AP, the spectroscopic properties of the nucleoside analog were only marginally affected by the phosphate group as well as the 2′-OH group (Table 1 and Figure 5), indicating that the phosphate and the 2′-OH groups do not significantly affect the fluorophore, at least in water.

### Thermodynamic stability of the 8vdA-labeled oligonucleotides in the duplex state

8vdA was incorporated in three 15mer oligonucleotides (ODN1–ODN3) of the type d(CGT TTT **XNX** TTT TGC), where N = 8vdA and X = T, A, and C for ODN1, ODN2 and ODN3, respectively. The oligonucleotide sequences were designed to be structureless [as predicted from the mfold program (50)] and not autocomplementary. Moreover, the sequences differed by the residues flanking the modified nucleotide since these residues were shown to play a critical role on the fluorescence properties of 2AP (51). In order to compare the properties of 8vdA and 2AP, the same oligonucleotides were prepared with 2AP.

As a first step to characterize the 8vdA- and 2AP-containing oligonucleotides, the thermodynamic stability of their duplexes was compared with the stability of the corresponding unlabeled duplexes by monitoring the temperature-induced absorbance changes at 260 nm (Table 2). As expected, comparison of the unlabeled sequences reveals that the most stable duplex is obtained with ODN3 in which the central A-T base pair is flanked by two stable G-C base pairs. $T_m$ measurements further indicate that 8vdA destabilizes the duplexes by only 0.4 and 1.5°C with respect to the unlabeled oligonucleotides when its flanking residues were T or A, respectively. This destabilization is significantly less than the 2.2 and 3.7°C decrease observed with the corresponding 2AP-labeled oligonucleotides (Table 2), or than the 5–6°C $T_m$ decrease reported when A is substituted by 8-methoxy-2′-deoxyadenosine (8moA) or 8-Bromo-2′-deoxyadenosine (8BrA) in oligonucleotides of comparable length (26). A reverse situation was observed when the chromophore was flanked by C residues since the 4.1°C decrease in $T_m$ with 8vdA was larger than that observed with 2AP. Similar conclusions were obtained when $\Delta G$ values were compared. Indeed, the free energy of the 8vdA-containg duplexes was −0.6 and −0.7 kcal/mol less than the 2AP-containing derivatives when the flanking residues were T or A, respectively, while it differed by +1 kcal/mol

**Table 2.** Thermodynamic parameters for duplex formation by the native and labeled oligonucleotides as monitored from the absorbance at 260 nm[a]

| | $T_m \pm 0.5$ (°C) | $\Delta T_m \pm 1$ (°C) | $\Delta G^0_{37}$ (kcal/mol) |
|---|---|---|---|
| ODN1 | 39.3 | | −10.5 |
| 8vdA-ODN1 | 38.9 | 0.4 | −10.2 |
| 2AP-ODN1 | 37.1 | 2.2 | −9.6 |
| ODN2 | 39.7 | | −10.6 |
| 8vdA-ODN2 | 38.2 | 1.5 | −10.0 |
| 2AP-ODN2 | 36.0 | 3.7 | −9.3 |
| ODN3 | 42.4 | | −11.5 |
| 8vdA-ODN3 | 38.3 | 4.1 | −10.1 |
| 2AP-ODN3 | 41.2 | 1.2 | −11.1 |

[a]The thermodynamic parameters were deduced from the melting curves, as described in the Materials and Methods section.

**Table 3.** Thermodynamic parameters for mismatch-containing duplexes[a]

| Sequence | Y | $\Delta T_m \pm 1$ (°C) N = A | N = 8vdA |
|---|---|---|---|
| ODN1 | A | 8 | 6 |
| | G | 6 | 8 |
| | C | 7 | 6 |
| ODN2 | A | 10 | 9 |
| | G | 9 | 10 |
| | C | 10 | 9 |
| ODN3 | A | 8 | 7 |
| | G | 6 | 6 |
| | C | 3 | 6 |

[a]Y designates the nature of the mismatched residue in the complementary sequences of ODN1–ODN3. The melting temperature decreases, $\Delta T_m$, for both 8-vdA labeled and unlabeled oligonucleotides correspond to the difference between the $T_m$ of the mismatch-containing duplex with the $T_m$ of the corresponding canonical (N = A, Y = T) duplex.

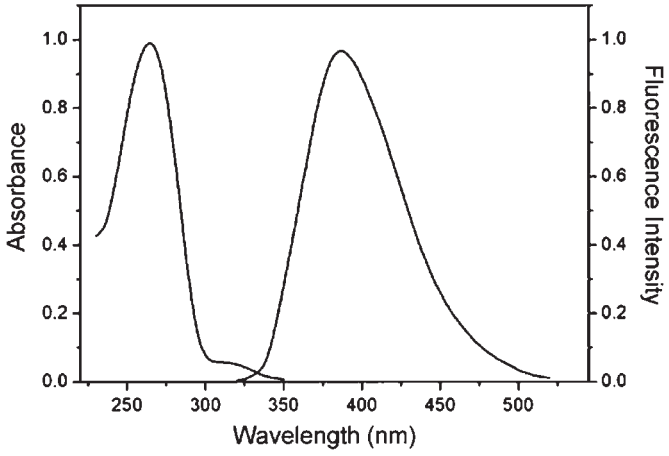


**Figure 6.** Absorption and emission spectra of ss8vdA-ODN1. The oligonucleotide was dissolved in HEPES 25 mM, NaCl 30 mM and $MgCl_2$ 0.2 mM, pH 7.5 at a concentration of 5.5 μM. The excitation wavelength for the emission spectrum was 305 nm.

when the flanking residues were C. Since the $T_m$ decrease observed with 8vdA in ODN1 and ODN2 is much less than the $T_m$ decrease usually observed with 8moA and 8BrA, which favor the *syn* conformation at the N-glycosidic bond, 8vdA may favor the *anti* conformation and form a canonical Watson–Crick base pair with the T residue in the complementary strand of these duplexes (52). In contrast, the rather large destabilization observed with 8vdA in ODN3 raises the possibility that the *anti* conformation of 8vdA, which is required for Watson–Crick base pairing, may be disfavored.

To further address the ability of 8vdA to form Watson–Crick or alternate base pairs, the T residue in the complementary strands of ODN1–ODN3 was substituted by a mismatched residue (Y = A, C or G) and the destabilization of the 8vdA-labeled duplexes was compared with the destabilization of the unlabeled duplexes (Table 3). Substitution of the central A-T base pair in the unlabeled ODN1 duplex by a mismatched A-Y pair induced a $T_m$ decrease of about 6–8°C. A very similar $T_m$ decrease was observed when the 8vdA-T pair was substituted by a 8vdA-Y pair, confirming that 8vdA behaves as A and very likely forms a Watson–Crick base pair with T in the ODN1 duplex. A similar conclusion applies also for ODN2 since similar $T_m$ decreases were observed for A and 8vdA when the complementary T residue was substituted by a mismatched residue. For ODN3, substitution of T by either A or G in the complementary sequence of the unlabeled sequence induced a 6–8°C decrease in $T_m$ while only a 3°C decrease in $T_m$ accompanied the substitution of T by C, suggesting that H bonds may stabilize the A-C pair. In labeled ODN3, where a rather large destabilization was measured when 8vdA is paired opposite T (4°C, Table 2), a more pronounced $T_m$ decrease was observed in mismatched pairs (6–7°C, Table 3) still indicating a preference for 8vdA being paired opposite T rather than A, G or C.

## Spectroscopic properties of 8vdA in single- and double-stranded oligonucleotides

To further assess the potential use of 8vdA as a fluorescent analog of deoxyadenosine, we characterized the spectroscopic properties of 8vdA in the ODN1–ODN3 oligonucleotides either in their single-stranded or in their duplex states. These properties were compared with those of 2AP in the same sequences.

Absorption and emission spectra of 8vdA in the single-stranded form of ODN1 are given in Figure 6. The absorption spectrum exhibits a broad absorption band with a maximum at 265 nm due to the native DNA bases and a shoulder centered at 310 nm (±5 nm) due to 8vdA absorption. The ratio of the absorbances A(310)/A(265) is close to the 1:15 ratio expected from the extinction coefficients of the bases and 8vdA, confirming that the sequences are stoichiometrically labeled. The emission spectrum of 8vdA in ODN1 with a maximum at 387 nm was found to be qualitatively similar to that of the 8vdA monomer. In sharp contrast, its quantum yield dropped dramatically (Table 4). This change in the quantum yield was accompanied by a dramatic increase in the complexity of the intensity decay, since up to four lifetimes were necessary to describe the 8vdA decay in ODN1. The major lifetime is the 70 ps component whose relative amplitude is about 50%, while the less quenched lifetime (3.4 ns) represents only 1%. The $7.7 \times 10^7$ $s^{-1}$ value of $k_r$ is two times lower than that of the 8vdA monomer, suggesting static quenching. In addition, $k_{nr}$ is increased by about two orders of magnitude with respect to the monomer, suggesting a strong increase in dynamic quenching. Furthermore, the duplex formation blue-shifted the emission spectrum of the 8vdA-labeled ODN1 by about 5 nm without any significant change in the quantum yield or time-resolved parameters suggesting that the spectroscopic behavior of 8vdA is mainly governed by intra-strand factors.

From the comparison with the 2AP-labeled ODN1 derivative, it appears that the 27-fold drop in the quantum yield of 8vdA in ODN-1 with respect to the free nucleoside was significantly less than the 40-fold drop observed with the corresponding 2AP-labeled derivative (Table 4). Interestingly, the number of lifetime components and the relative amplitudes of the corresponding lifetimes were similar in the two labeled oligonucleotides. In fact, only the lifetime values differed somewhat, those of the 2AP-labeled derivative being higher than the corresponding lifetimes in the 8vdA-labeled

**Table 4.** Steady-state and time-resolved fluorescence parameters of 8vdA- and 2AP-labeled oligonucleotides[a]

| | $\lambda_{em}$ nm | $\phi \pm 0.005$ | $\tau_1$ (ns) | $\alpha_1$ | $\tau_2$ (ns) | $\alpha_2$ | $\tau_3$ (ns) | $\alpha_3$ | $\tau_4$ (ns) | $\alpha_4$ | $<\tau>$ (ns) $\pm$ 0.03 | $k_f(10^7\ s^{-1}) \pm 1 \times 10^7$ | $k_{nr}\ (10^9\ s^{-1}) \pm 0.5 \times 10^9$ |
|---|---|---|---|---|---|---|---|---|---|---|---|---|---|
| ss8vdA-ODN1 | 387 | 0.024 | 0.071 | 0.52 | 0.22 | 0.34 | 1.23 | 0.13 | 3.42 | 0.012 | 0.31 | 7.7 | 3.1 |
| ds8vdA-ODN1 | 382 | 0.028 | 0.053 | 0.42 | 0.19 | 0.38 | 1.33 | 0.19 | 3.05 | 0.003 | 0.36 | 7.8 | 2.7 |
| ss2AP-ODN1 | 372 | 0.017 | 0.065 | 0.52 | 0.31 | 0.27 | 1.58 | 0.17 | 4.21 | 0.045 | 0.58 | 2.9 | 1.7 |
| ds2AP-ODN1 | 369 | 0.016 | 0.079 | 0.28 | 0.45 | 0.69 | 1.56 | 0.023 | 4.87 | 0.0061 | 0.40 | 4.0 | 2.5 |
| ss8vdA-ODN2 | 388 | 0.014 | 0.16 | 0.81 | 0.64 | 0.14 | 1.63 | 0.044 | 4.39 | 0.009 | 0.33 | 4.2 | 3.0 |
| ds8vdA-ODN2 | 383 | 0.016 | 0.15 | 0.73 | 0.35 | 0.19 | 1.32 | 0.081 | 3.85 | 0.0058 | 0.30 | 5.3 | 3.3 |
| ss2AP-ODN2 | 372 | 0.010 | 0.15 | 0.72 | 1.10 | 0.19 | 2.66 | 0.09 | 6.14 | 0.0015 | 0.57 | 1.8 | 1.7 |
| ds2AP-ODN2 | 369 | 0.012 | 0.17 | 0.86 | 0.58 | 0.084 | 2.27 | 0.044 | 6.75 | 0.012 | 0.37 | 3.2 | 2.7 |
| ss8vdA-ODN3 | 389 | 0.037 | 0.20 | 0.64 | 0.89 | 0.28 | 1.99 | 0.076 | 4.02 | 0.0089 | 0.56 | 6.6 | 1.7 |
| ds8vdA-ODN3 | 384 | 0.005 | 0.055 | 0.94 | 0.29 | 0.032 | 1.40 | 0.016 | 2.62 | 0.0083 | 0.11 | 4.6 | 9.0 |
| ss2AP-ODN3 | 371 | 0.020 | 0.16 | 0.69 | 0.92 | 0.16 | 1.96 | 0.13 | 4.85 | 0.019 | 0.61 | 3.3 | 1.6 |
| ds2AP-ODN3 | 369 | 0.003 | 0.044 | 0.96 | 0.34 | 0.015 | 1.44 | 0.011 | 3.76 | 0.0089 | 0.10 | 3.0 | 9.9 |

[a]The fluorescence lifetimes, $\tau_i$, the relative amplitudes, $\alpha_i$, and the mean lifetime, $<\tau>$, are expressed as means for at least two experiments. ss and ds represent respectively the single-strand and double-strand states of the different oligonucleotides.

derivative. Moreover, the duplex formation of the 2AP-labeled oligonucleotide induces only limited changes in both the steady-state parameters and lifetime values as with the 8vdA-labeled oligonucleotide.

The data with the labeled ODN2 derivatives were similar to those of the ODN1 derivatives, except that the quantum yield of both dyes was significantly lower in ODN2 than in ODN1. In addition, the quantum yield of 8vdA was again higher (40%) than that of 2AP in ODN2. Moreover, the values of the four lifetime components of 8vdA were systematically higher in ODN2 than in ODN1, suggesting that these values are strongly dependent on the interaction with the flanking residues. A similar conclusion applies for the fractional populations associated with the lifetimes since notably the population associated with $\tau_1$ was much larger in ODN2 than in ODN1 for both dyes.

Finally, the most interesting results were obtained with ODN3. The quantum yield of 8vdA was much higher in ODN3 than in ODN1 and ODN2 and was about twice the quantum yield of the 2AP-labeled ODN3 derivative. This suggests that 8vdA was less quenched by C than by A or T residues and that 2AP was more strongly quenched by C residues than 8vdA. The higher quantum yield of 8vdA in ODN3 as compared to ODN1 and ODN2 is mainly related to a decrease in $k_{nr}$ and thus to a decrease in dynamic quenching. In contrast to ODN1 and ODN2, the lifetimes of 8vdA and 2AP were similar in ODN3. Remarkably, duplex formation dramatically decreases the quantum yield and lifetimes (mainly by increasing the $k_{nr}$ values) of both 8vdA and 2AP in ODN3, implying that both probes could sensitively monitor duplex formation in this case.

## DISCUSSION

We reported herein an efficient approach for the synthesis of the sensitive 8vdA phosphoramidite. Using fast deprotecting groups and several modifications in standard solid phase chemistry, we have integrated this building block in different oligonucleotide sequences and have optimized deprotection conditions to obtain the amount of products required for thermal denaturation and fluorescence studies.

Introduction of 8vdA in the central position of the ODN1 and ODN2 oligonucleotides induces only a marginal decrease in the melting temperature and free energy of the duplexes with respect to the corresponding canonical duplexes (Table 2). In addition, when the abilities of 8vdA and A to pair opposite mismatches were compared (Table 3), the strikingly similar $T_m$ decreases strongly suggest that, as expected from its structural similarity with deoxyadenosine, 8vdA adopts an *anti* conformation to preserve Watson–Crick hydrogen bonding with the T residue on the opposite strand in the duplex. The decrease in $T_m$ and free energy induced by 8vdA was even less than with 2AP in both ODN1 and ODN2. This may be rationalized by the displacement from the position 6 to position 2 of the exocyclic amino group in 2AP, but not in 8vdA, that locally changes the duplex structure by moving one of the H bonds from the major to the minor groove (4). The greater duplex destabilization observed with the 8vdA-labeled ODN3 might result from a greater steric penalty of the vinyl substituent and/or from the disruption of the spine of hydration in the major groove (27,53). Thus, the influence of 8vdA on the duplex stability is dictated both by the base pair and the sequence context. A similar conclusion also holds for 2AP, as can be seen from the data in Table 2. By analogy to 2AP, the quantum yield of 8vdA dramatically drops when it is included in an oligonucleotide. However, in the three tested oligonucleotides, the quantum yield of 8vdA was higher than that of 2AP, the difference being up to a factor of two. The difference in emission between the two labels is further exalted by the higher absorption coefficient of 8vdA with respect to 2AP. Indeed, though the absorption spectrum of 8vdA is shifted by about 13 nm to the blue with respect to that of 2AP, its absorption coefficients in the 300–310 nm range (where the absorption of the natural bases is insignificant) are 1.1–1.9 higher than those of 2AP. As a consequence, 8vdA appears as a better fluorescent analog than 2AP.

The photophysics of 8vdA and 2AP in the oligonucleotides are probably similar since the time-resolved parameters and the quantum yield of the two analogs exhibit similar dependency on the nature of the flanking residues and strands. In this respect, by analogy to 2AP (3,8,10), the multiple lifetime components of 8vdA in oligonucleotides may reflect a distribution of local conformations in which 8vdA experiences varying degrees of stacking with the flanking residues within the same strand. The small amplitude and lifetime values of the least-stacked form of 8vdA in the three tested

oligonucleotides further suggest that 8vdA experiences only limited displacement relative to its neighbors. In addition, incorporation of 8vdA in oligonucleotides induces a marked decrease in its radiative rate constant, as for 2AP, in line with a mechanism of static quenching due to electron delocalization in the ground state with a loss of oscillator strength (51,54). Furthermore, the large increase in the nonradiative rate constant as well as the appearance of several short-lived lifetimes may result, as in the case of 2AP, from a dynamic quenching with loss of energy via nonradiative relaxation to one or more charge transfer states, which are absent in free 8vdA (51,54).

The limited changes in 2AP and 8vdA fluorescence parameters associated with the formation of ODN1 and ODN2 duplexes suggest that the photophysics as well as the stacking of 8vdA with its closest neighbors are not affected by the complementary strand. In contrast, the dramatic changes observed with ODN3 suggest that hydrogen bonding to the opposing residue may reinforce the π-stacking interactions of 8vdA with the neighboring bases in this case.

Taken together, our data indicate that 8vdA may be used as an alternative to 2AP, to fluorescently label oligonucleotides. Due to the sensitivity of its fluorescence to solvent, temperature and flanking bases, it may be used for the same applications than 2AP, with an improved sensitivity due to its higher extinction coefficient and quantum yield. On the other hand, in duplexes containing 2AP, one hydrogen bond is moved from the major to the minor groove whereas in 8vdA-labeled duplexes where the *anti* conformation is favored, the hydrogen bonding pattern remains unchanged. This might be of prime importance for some specific applications such as studies of DNA replication fidelity (55). Moreover, since the position 8 offers larger possibilities of chemical modifications than the position 2 on the purine base, further improvements in the chemical and photophysical properties may in principle be achieved. Experiments are currently being performed to further assess the potency of 8vdA as a fluorescent probe.

## SUPPLEMENTARY MATERIAL

Supplementary Material is available at NAR Online.

## ACKNOWLEDGEMENTS

This work was supported by grants from the Agence Nationale de Recherches sur le SIDA (ANRS), Sidaction (Ensemble Contre le Sida), Université Louis Pasteur and the European Community (TRIoH integrated project). H.B. and N.B.G. were fellows from the Ministère de la Recherche et des Technologies. Funding to pay the Open Access publication charges for this article was provided by TRIoH.

## REFERENCES

1. Mollova,E.T. (2002) Single-molecule fluorescence of nucleic acids. *Curr. Opin. Chem. Biol.*, **6**, 823–828.
2. Ward,D.C., Reich,E. and Stryer,L. (1969) Fluorescence studies of nucleotides and polynucleotides. I. Formycin, 2-aminopurine riboside, 2,6-diaminopurine riboside, and their derivatives. *J. Biol. Chem.*, **244**, 1228–1237.
3. Nordlund,T.M., Andersson,S., Nilsson,L., Rigler,R., Graslund,A. and McLaughlin,L.W. (1989) Structure and dynamics of a fluorescent DNA oligomer containing the EcoRI recognition sequence: fluorescence, molecular dynamics, and NMR studies. *Biochemistry*, **28**, 9095–9103.
4. Sowers,L.C., Fazakerley,G.V., Eritja,R., Kaplan,B.E. and Goodman,M.F. (1986) Base pairing and mutagenesis: observation of a protonated base pair between 2-aminopurine and cytosine in an oligonucleotide by proton NMR. *Proc. Natl Acad. Sci. USA*, **83**, 5434–5438.
5. Sowers,L.C., Eritja,R., Chen,F.M., Khwaja,T., Kaplan,B.E., Goodman,M.F. and Fazakerley,G.V. (1989) Characterization of the high pH wobble structure of the 2-aminopurine:cytosine mismatch by nitrogen-15 NMR spectroscopy. *Biochem. Biophys. Res. Commun.*, **165**, 89–92.
6. Fagan,P.A., Fabrega,C., Eritja,R., Goodman,M.F. and Wemmer,D.E. (1996) NMR study of the conformation of the 2-aminopurine:cytosine mismatch in DNA. *Biochemistry*, **35**, 4026–4033.
7. Nordlund,T.M., Xu,D. and Evans,K.O. (1993) Excitation energy transfer in DNA: duplex melting and transfer from normal bases to 2-aminopurine. *Biochemistry*, **32**, 12090–12095.
8. Rachofsky,E.L., Seibert,E., Stivers,J.T., Osman,R. and Ross,J.B.A. (2001) Conformation and dynamics of abasic sites in DNA investigated by time-resolved fluorescence of 2-aminopurine. *Biochemistry*, **40**, 957–967.
9. Stivers,J.T. (1998) 2-Aminopurine fluorescence studies of base stacking interactions at abasic sites in DNA: metal-ion and base sequence effects. *Nucleic Acids Res.*, **26**, 3837–3844.
10. Guest,C.R., Hochstrasser,R.A., Sowers,L.C. and Millar,D.P. (1991) Dynamics of mismatched base pairs in DNA. *Biochemistry*, **30**, 3271–3279.
11. Menger,M., Tuschl,T., Eckstein,F. and Porschke,D. (1996) $Mg^{2+}$-dependent conformational changes in the hammerhead ribozyme. *Biochemistry*, **35**, 14710–14716.
12. Bandwar,R.P. and Patel,S.S. (2001) Peculiar 2-aminopurine fluorescence monitors the dynamics of open complex formation by bacteriophage T7 RNA polymerase. *J. Biol. Chem.*, **276**, 14075–14082.
13. Ujvari,A. and Martin,C.T. (1996) Thermodynamic and kinetic measurements of promoter binding by T7 RNA polymerase. *Biochemistry*, **35**, 14574–14582.
14. Jia,Y., Kumar,A. and Patel,S.S. (1996) Equilibrium and stopped-flow kinetic studies of interaction between T7 RNA polymerase and its promoters measured by protein and 2-aminopurine fluorescence changes. *J. Biol. Chem.*, **271**, 30451–30458.
15. Allan,B.W., Reich,N.O. and Beechem,J.M. (1999) Measurement of the absolute temporal coupling between DNA binding and base flipping. *Biochemistry*, **38**, 5308–5314.
16. Beechem,J.M., Otto,M.R., Bloom,L.B., Eritja,R., Reha-Krantz,L.J. and Goodman,M.F. (1998) Exonuclease-polymerase active site partitioning of primer-template DNA strands and equilibrium $Mg^{2+}$ binding properties of bacteriophage T4 DNA polymerase. *Biochemistry*, **37**, 10144–10155.
17. Raney,K.D., Sowers,L.C., Millar,D.P. and Benkovic,S.J. (1994) A fluorescence-based assay for monitoring helicase activity. *Proc. Natl Acad. Sci. USA*, **91**, 6644–6648.
18. Holz,B., Klimasauskas,S., Serva,S. and Weinhold,E. (1998) 2-Aminopurine as a fluorescent probe for DNA base flipping by methyltransferases. *Nucleic Acids Res.*, **26**, 1076–1083.
19. Baliga,R., Baird,E.E., Herman,D.M., Melander,C., Dervan,P.B. and Crothers,D.M. (2001) Kinetic consequences of covalent linkage of DNA binding polyamides. *Biochemistry*, **40**, 3–8.
20. Rist,M. and Marino,J. (2001) Association of an RNA kissing complex analyzed using 2-aminopurine fluorescence. *Nucleic Acids Res.*, **29**, 2401–2408.
21. Rist,M.J. and Marino,J.P. (2002) Mechanism of nucleocapsid protein catalyzed structural isomerization of the dimerization initiation site of HIV-1. *Biochemistry*, **41**, 14762–14770.
22. Saenger,W. (1984) *Principles of Nucleic Acid Structure*. Springer-Verlag, NY.
23. Abdallah,M.A., Biellmann,J.-F., Nordström,B. and Brändén,C.-I. (1975) The conformation of adenosine diphosphoribose and 8-bromoadenosine diphosphoribose when bound to liver alcohol dehydrogenase. *Eur. J. Biochem.*, **50**, 475–481.
24. Limn,W., Uesugi,S., Ikehara,M. and Miles,H.T. (1983) Poly (8-methyladenylic acid): a single-stranded regular structure with

alternating syn-anti conformations. *Biochemistry*, **22**, 4217–4222.
25. Dias,E., Battiste,J.L. and Williamson,J.R. (1994) Chemical probe for glycosidic conformation in telomeric DNAs. *J. Am. Chem. Soc.*, **116**, 4479–4480.
26. Eason,R.G., Burkhardt,D.M., Phillips,S.J., Smith,D.P. and David,S.S. (1996) Synthesis and characterization of 8-methoxy-2′-deoxyadenosine-containing oligonucleotides to probe the syn glycosidic conformation of 2′-deoxyadenosine within DNA. *Nucleic Acids Res.*, **24**, 890–897.
27. Seela,F. and Zulauf,M. (1998) 7-Deaza-adenine-DNA: bulky 7-iodo substituents or hydrophobic 7-hexynyl chains are well accommodated in the major groove of oligonucleotide duplexes. *Chem. Eur. J.*, **4**, 1781–1790.
28. Booth,J., Cummins,W.J. and Brown,T. (2004) An analogue of adenine that forms an ''A:T'' base pair of comparable stability to G:C. *Chem. Commun.*, pp. 2208–2209.
29. Breslauer,K.J. (1995) Extracting thermodynamic data from equilibrium melting curves for oligonucleotide order-disorder transitions. *Methods Enzymol.*, **259**, 221–242.
30. Ramos,P., Coste,T., Piemont,E., Lessinger,J.M., Bousquet,J.A., Chapus,C., Kerfelec,B., Ferard,G. and Mely,Y. (2003) Time-resolved fluorescence allows selective monitoring of Trp30 environmental changes in the seven-Trp-containing human pancreatic lipase. *Biochemistry*, **42**, 12488–12496.
31. Livesey,A.K. and Brochon,J.C. (1987) Analyzing the distribution of decay constants in pulse-fluorimetry using the maximum entropy method. *Biophys. J.*, **52**, 693–706.
32. Manfredini,S., Baraldi,P.G., Bazzanini,R., Marangoni,M., Simoni,D., Balzarini,J. and De Clercq,E. (1995) Synthesis and cytotoxic activity of 6-vinyl- and 6-ethynyluridine and 8-vinyl- and 8-ethynyladenosine. *J. Med. Chem.*, **38**, 199–203.
33. Van Aerschot,A.A., Mamos,P., Weyns,N.J., Ikeda,S., De Clercq,E. and Herdewijn,P.A. (1993) Antiviral activity of C-alkylated purine nucleosides obtained by cross-coupling with tetraalkyltin reagents. *J. Med. Chem.*, **36**, 2938–2942.
34. Liu,F., Dalhus,B., Gundersen,L.-L. and Rise,F. (1999) Addition and cycloaddition to 2- and 8-vinylpurines. *Acta Chem. Scand.*, **53**, 269–279.
35. Lang,P., Gerez,C., Tritsch,D., Fontecave,M., Biellmann,J.-F. and Burger,A. (2003) Synthesis of 8-vinyladenosine 5′-di- and 5′-triphosphate: evaluation of the diphosphate compound on ribonucleotide reductase. *Tetrahedron*, **59**, 7315–7322.
36. Tierney,M.T. and Grinstaff,M.W. (2000) Synthesis and stability of oligodeoxynucleotides containing C8-labeled 2′-deoxyadenosine: novel redox nucleobase probes for DNA-mediated charge-transfer studies. *Org. Lett.*, **2**, 3413–3416.
37. Graham,D., Parkinson,J.A. and Brown,T. (1998) DNA duplexes stabilized by modified monomer residues: synthesis and stability. *J. Chem. Soc. [Perkin Trans. 1]*, pp. 1131–1138.
38. Froehler,B.C. and Matteucci,M.D. (1983) Dialkylformamidines: depurination resistant N6-protecting group for deoxyadenosine. *Nucleic Acids Res.*, **11**, 8031–8036.
39. Sinha,N.D., Davis,P., Usman,N., Perez,J., Hodge,R., Kremsky,J. and Casale,R. (1993) Labile exocyclic amine protection of nucleosides in DNA, RNA and oligonucleotide analog synthesis facilitating N-deacylation, minimizing depurination and chain degradation. *Biochimie*, **75**, 13–23.
40. Vu,H., McCollum,C., Jacobson,K., Theisen,P., Vinayak,R., Spiess,E. and Andrus,Alex (1990) Fast oligonucleotide deprotection phosphoramidite chemistry for DNA synthesis. *Tetrahedron Lett.*, **31**, 7269–7272.
41. Septak,M. (1996) Kinetic studies on depurination and detritylation of CPG-bound intermediates during oligonucleotide synthesis. *Nucleic Acids Res.*, **24**, 3053–3058.
42. Zhu,Q., Delaney,M.O. and Greenberg,M.M. (2001) Observation and elimination of N-acetylation of oligonucleotides prepared using fast-deprotecting phosphoramidites and ultra-mild deprotection. *Bioorg. Med. Chem. Lett.*, **11**, 1105–1107.
43. Wu,T., Ogilvie,K.K. and Pon,R.T. (1989) Prevention of chain cleavage in the chemical synthesis of 2′-silylated oligoribonucleotides. *Nucleic Acids Res.*, **17**, 3501–3517.
44. Schulhof,J.C., Molko,D. and Teoule,R. (1987) The final deprotection step in oligonucleotide synthesis is reduced to a mild and rapid ammonia treatment by using labile base-protecting groups. *Nucleic Acids Res.*, **15**, 397–416.
45. Kataoka,M., Hattori,A., Okino,S., Hyodo,M., Asano,M., Kawai,R. and Hayakawa,Y. (2001) Ethyl(methyl)dioxirane as an efficient reagent for the oxidation of nucleoside phosphites into phosphates under nonbasic anhydrous conditions. *Org. Lett.*, **3**, 815–818.
46. McBride,L.J., Kierzek,R., Beaucage,S.L. and Caruthers,M.H. (1986) Nucleotide chemistry. 16. Amidine protecting groups for oligonucleotide synthesis. *J. Am. Chem. Soc.*, **108**, 2040–2048.
47. Nagatsugi,F., Uemura,K., Nakashima,S., Maeda,M. and Sasaki,S. (1997) 2-Aminopurine derivatives with C6-substituted olefin as novel crosslinking agents and the synthesis of the corresponding beta-phosphoramidite precursors. *Tetrahedron*, **53**, 3035–3044.
48. Rinkel,L.J. and Altona,C. (1987) Conformational analysis of the deoxyribofuranose ring in DNA by means of sums of proton-proton coupling constants: a graphical method. *J. Biomol. Struct. Dyn.*, **4**, 621–649.
49. Rosemeyer,H., Toth,G., Golankiewicz,B., Kazimierczuk,Z., Bourgeois,W., Kretschmer,U., Muth,H.P. and Seela,F. (1990) Syn-anti conformational analysis of regular and modified nucleosides by 1D 1H NOE difference spectroscopy: a simple graphical method based on conformationally rigid molecules. *J. Org. Chem.*, **55**, 5784–5790.
50. SantaLucia,J.,Jr (1998) A unified view of polymer, dumbbell, and oligonucleotide DNA nearest-neighbor thermodynamics. *Proc. Natl Acad. Sci. USA*, **95**, 1460–1465.
51. Jean,J.M. and Hall,K.B. (2001) 2-Aminopurine fluorescence quenching and lifetimes: role of base stacking. *Proc. Natl Acad. Sci. USA*, **98**, 37–41.
52. Law,S.M., Eritja,R., Goodman,M.F. and Breslauer,K.J. (1996) Spectroscopic and calorimetric characterizations of DNA duplexes containing 2-aminopurine. *Biochemistry*, **35**, 12329–12337.
53. Hashimoto,H., Nelson,M.G. and Switzer,C. (1993) ZwitterioniC DNA. *J. Am. Chem. Soc.*, **115**, 7128–7134.
54. Jean,J.M. and Hall,K.B. (2002) 2-Aminopurine electronic structure and fluorescence properties in DNA. *Biochemistry*, **41**, 13152–13161.
55. Kunkel,T.A. and Bebenek,K. (2000) DNA replication fidelity. *Annu. Rev. Biochem.*, **69**, 497–529.